Catalysis Today 149 (2010) 163–166

Contents lists available at ScienceDirect

Catalysis Today

journal homepage: www.elsevier.com/locate/cattod

Effect of Pd loading and precursor on the catalytic performance of $Pd/WO_3–ZrO_2$ catalysts for selective oxidation of ethylene

Lixia Wang [a,b], Shuliang Xu [a,b], Wenling Chu [a,*], Weishen Yang [a,*]

[a] State Key Laboratory of Catalysis, Dalian Institute of Chemical Physics, Chinese Academy of Sciences, 457 Zhongshan Road, Dalian 116023, China
[b] Graduate School of the Chinese Academy of Sciences, China

ARTICLE INFO

Article history:
Available online 5 April 2009

Keywords:
$Pd/WO_3–ZrO_2$
Pd loading
Pd precursors
Polytungstates
Pd species

ABSTRACT

The structure and properties of $Pd/WO_3–ZrO_2$ (W/Zr = 0.2) catalysts with different Pd loadings and precursors were investigated. The results indicate that $Pd/WO_3–ZrO_2$ prepared from a $PdCl_2$ precursor was optimum for high activity and selectivity. Moreover, ethylene conversion increased with the Pd loading. The structure and nature of the catalysts were characterized using X-ray diffraction, BET N_2 adsorption, H_2 temperature-programmed reduction and H_2 pulse adsorption techniques. The results reveal that the higher catalytic performance of $Pd/WO_3–ZrO_2$ prepared from $PdCl_2$ could be related to the formation of polytungstate species and the existence of well-dispersed Pd particles.

1. Introduction

In recent years, there has been a pronounced tendency to use one-step ethylene oxidation as an alternative method to produce acetic acid. In the early stages of development, a number of Pd-containing solid acid catalysts were investigated [1–3]. Unfortunately, the catalytic performance of Pd-containing solid acid catalysts, such as $Pd–Cr_2O_3/Al_2O_3$ [1], $Pd–V_2O_5–Sb_2O_5/Al_2O_3$ [2] and $Pd–H_3PO_4/SiO_2$ [3], is rather poor. Thus, many investigations have been carried out to develop a promising catalyst.

In 1997, Showa Denko K.K. commercialized the process of ethylene oxidation to acetic acid using palladium-based heteropolyacid catalysts [4], for which a significantly higher acetic acid yield ($\sim$100 g L^{-1} h^{-1}) was reported for $Pd–H_4SiW_{12}O_{40}/SiO_2$ as the catalyst. In all these examples, a common feature of the catalysts for selective ethylene oxidation is that bi-functional catalysts comprising palladium and an acidic support appear to favor the selective formation of acetic acid [4]. Accordingly, it is expected that solid acid supports other than $H_4SiW_{12}O_{40}/SiO_2$ will also show excellent catalytic performance in combination with Pd.

It has been reported that Pd supported on $WO_3–ZrO_2$ catalysts exhibit high catalytic activity for selective ethylene oxidation at 423 K [5,6]. In the present study, we investigated the effect of the Pd loading and precursor on the catalytic performance for ethylene oxidation. Structural analysis of the catalysts was performed using X-ray diffraction (XRD), BET N_2 adsorption and H_2 temperature-programmed reduction (TPR) techniques and the results were correlated with the catalytic performance.

2. Experimental

2.1. Catalyst preparation

$WO_3–ZrO_2$ catalysts with a W/Zr ratio of 0.2 were prepared using a previously reported procedure [5]. Pd was impregnated on the $WO_3–ZrO_2$ support using a wet impregnation method and the Pd loading was varied from 0.5 to 2.0 wt.%. To investigate the influence of the Pd precursor, $PdCl_2$, $Pd(NH_3)_2Cl_2$ and $Pd(CH_3COO)_2$ were used. After drying at 373 K, the resulting solids were calcined at 673 K in static air for 5 h.

2.2. Catalyst characterization

The specific surface area and pore size distribution of the catalysts were measured by nitrogen adsorption/desorption at 77 K using a Counter Omnisorp-100CX system. Samples were first degassed at 623 K under high vacuum (1.33×10^{-4} Pa) for 3 h before isotherms were recorded.

Powder XRD patterns were recorded on a Rigaku D/Max-2500 diffractometer using Cu Kα radiation (λ = 0.1542 nm) in the 2θ range 10–90° at a scan rate of 0.02° s^{-1} at 40 kV and 200 mA.

TPR was carried out on freshly prepared catalysts to identify reducible species on the catalyst surface. The analysis was conducted on a homemade apparatus. In a typical experiment, 0.05 g of sample was purged with flowing He at 373 K for 1 h and

---

[*] Corresponding authors. Tel.: +86 411 84379073; fax: +86 411 84694447.
E-mail addresses: cwl@dicp.ac.cn (W. Chu), Yangws@dicp.ac.cn (W. Yang).
URL: http://yanggroup.dicp.ac.cn

0920-5861/$ – see front matter © 2009 Elsevier B.V. All rights reserved.
doi:10.1016/j.cattod.2009.02.041

then cooled to room temperature prior to TPR experiments. The temperature was increased from room temperature to 1273 K at 10 K min^{-1} in a mixture of 5 mol% H_2/Ar. The rate of hydrogen consumption was detected by thermal conductivity detector (TCD) and recorded as the TPR profile of the catalyst.

Pd dispersion was measured using a H_2 pulse adsorption method on an Autosorb-1/C gas chemisorption system at 313 K. In a typical experiment, the sample was first pretreated in a He flow at 673 K for 2 h and subsequently reduced in H_2 gas at 573 K for 1 h. Then hydrogen was purged from the system by evacuation for 2 h. The adsorption isotherm was established by measuring the amount of H_2 adsorbed as a function of pressure at 313 K.

2.3. Catalytic performance

Oxidation of ethylene was performed in a fixed-bed flow reactor (stainless steel, 10 mm i.d.). A sample of 2 cm^3 of catalyst (3.6 g, 40–60 mesh) was placed in the reactor and pretreated at 573 K for 1 h under a stream of H_2–He (1:1 mixture) at a flow rate of 60 cm^3 min^{-1}. After cooling under a He flow to the reaction temperature of 423 K, a mixture of the reactant gas ($C_2H_4/O_2/H_2O$/He 50:7:30:13 by vol.) was fed into the reactor at a total flow rate of 100 cm^3 min^{-1} (SV = 3000 h^{-1}) and a total pressure of 0.6 MPa. A trap filled with water cooled with ice-water (~273 K) was used to collect the liquid products, which were analyzed by GC on an Agilent 6890 instrument equipped with an FFAP column and a flame ionization detector. Gaseous compounds were analyzed using an on-line TCD-GC instrument equipped with a Porapak Q column.

3. Results and discussion

3.1. Effect of Pd loading

The surface area of Pd/WO_3–ZrO_2 (W/Zr = 0.2) samples with Pd loading varying from 0.5 to 2.0 wt.% is listed in Table 1. The surface area of WO_3–ZrO_2 was found to be 46 m^2 g^{-1}. On the introduction of palladium, a decrease in surface area was observed due to pore blockage. However, when the Pd loading was increased from 0.5 to 2.0 wt.%, the BET surface area decreased slightly from 40 to 38 m^2 g^{-1}, implying that the increase in Pd loading has almost no effect on the BET surface area. The Pd dispersion and particle size were calculated from H_2 uptake data (listed in Table 1). The Pd dispersion on 0.5 wt.% Pd–WO_3/ZrO_2 was 22.8%, which was the highest among the catalysts. There were general tendencies for all the catalysts, with a decrease in Pd dispersion and a consequent increase in particle size when the Pd loading was increased from 0.5 to 2.0 wt.%.

XRD patterns (data not shown) of the Pd/WO_3–ZrO_2 catalysts with different Pd loadings exhibited peaks attributed to diffraction for the WO_3–ZrO_2 support alone [7], suggesting that Pd was present in a well-dispersed state on the support, and therefore small Pd particles could not be detected by XRD.

TPR profiles for catalysts with Pd content varying from 0.5 to 2.0 wt.% are shown in Fig. 1. The profiles reveal information about the variation in reduction temperature for Pd species with respect to Pd loading. It can be seen from Fig. 1 that the catalysts exhibited two types of peak related to Pd species. One is a negative peak at approximately 360 K that is characteristic of decomposition of the β-PdH phase [8], indicating the presence of metallic Pd particles [9]. The other is a peak for hydrogen consumption at ca. 410 K that can be attributed to the reduction of PdO species on the support [10]. Notably, no remarkable difference could be observed for the reduction peaks for metallic Pd and PdO species. This means that, for Pd loading of <2.0 wt.%, the Pd state is independent of the Pd loading. For the WO_3–ZrO_2 sample without any Pd, three reduction peaks were observed [11]. H_2 consumption at 773 K is probably attributable to polytungstate species or small WO_x clusters, and the other two peaks at significantly higher temperatures (973 and 1173 K) are assigned to the reduction of crystalline WO_3 oxides [12]. It is worth noting that the reduction peak due to polytungstate species (773 K) shifted to lower temperature (~613 K) for Pd-containing catalysts due to the interaction between palladium and the WO_3–ZrO_2 support. In particular, it is evident from Fig. 1 that the amount of polytungstate species at 613 K tended to increase as the Pd loading increased from 0.5 to 2.0 wt.%.

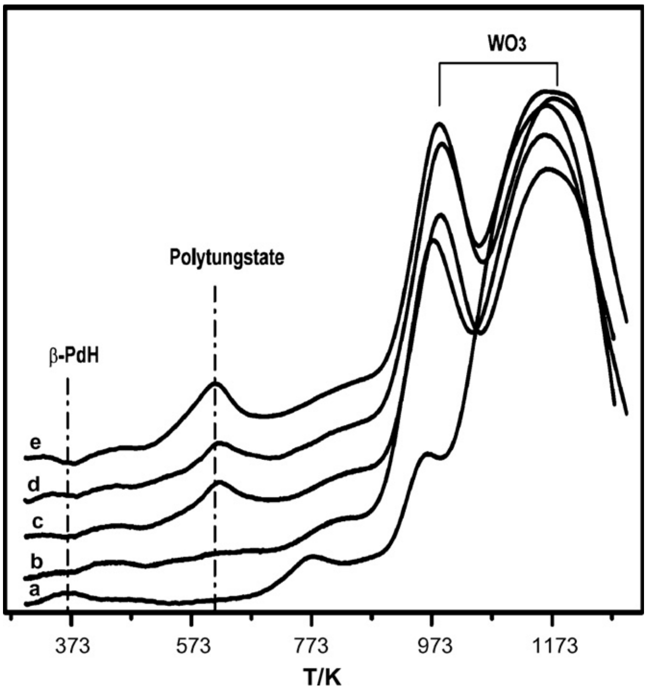

Fig. 1. H_2-TPR spectra of Pd/WO_3–ZrO_2 with different Pd loadings: (a) 0%; (b) 0.5%; (c) 1%; (d) 1.5%; (e) 2%.

Table 1 shows the effect of Pd loading on the catalytic performance of Pd/WO_3–ZrO_2 catalysts in the selective oxidation of ethylene. Pd-free WO_3–ZrO_2 exhibited almost no catalytic activity for the formation of acetic acid. Introduction of palladium dramatically increased the ethylene conversion and acetic acid

Table 1
Physical properties and catalytic performance of Pd/WO_3–ZrO_2 catalysts with various Pd loadings.

Pd loading (wt.%)	Surface area (m^2 g^{-1})	Pd dispersion (%)	Pd particle size (nm)	Ethylene conversion (%)	Acetic acid yield (g h^{-1} L^{-1} cat)	Selectivity (%)		
						Acetic acid	Acetaldehyde	CO_x
0.0	46	–	–	0.3	0.2	2	9	87
0.5	40	22.8	4.9	2.7	67	63	26	11
1.0	39	12.0	9.3	4.2	117	75	11	14
1.5	39	8.0	14.0	4.3	130	77	9	14
2.0	38	7.2	15.6	4.9	154	78	8	14

yield, further confirming that a bi-functional catalyst comprising palladium and an acidic support is favorable for the selective formation of acetic acid [4]. The catalytic activity (or yield of acetic acid) clearly increased as a function of Pd loading, with 2.0 wt.% Pd/WO_3–ZrO_2 exhibiting the highest ethylene conversion. Although Pd dispersion also varied with the Pd loading (Table 1), the difference in catalytic activity cannot be explained by this difference, suggesting that Pd dispersion is not responsible for the catalytic activity. Combining the H_2-TPR data and the results for catalytic activity, it is noteworthy that the ethylene conversion increased with the Pd content, in agreement with the polytungstate species trend at 613 K in Fig. 1. Based on this finding, we speculate that the presence of polytungstate species at 613 K plays an important role in increasing the activity of Pd-containing WO_3–ZrO_2 catalysts. On the other hand, the CO_x selectivity showed no obvious change when the Pd loading was increased from 0.5 to 2.0 wt.%, perhaps because of the similar Pd state. Only one significant difference in product distribution was observed: lower acetic acid and higher acetaldehyde selectivity for 0.5 wt.% Pd/WO_3–ZrO_2. The reason for this could be the lower Pd loading, which may not have been sufficient to oxidize the intermediate acetaldehyde to acetic acid.

3.2. Effect of Pd precursor

The above results indicate that the catalyst with 1.0 wt.% Pd loading exhibited satisfactory catalytic activity and acetic acid yield. Thus, to minimize the amount of Pd used for economic reasons, subsequent investigations focused on the 1.0 wt.% Pd/WO_3–ZrO_2 catalyst. The BET surface area and Pd dispersion calculated from H_2 chemisorption results for this catalyst prepared from different Pd precursors are summarized in Table 2. No appreciable change in BET surface area was observed, indicating that the Pd precursor has almost no influence on the textural structure of the catalysts. An interesting observation from the H_2 chemisorption results is that a change in palladium precursor yielded different Pd dispersion. Higher dispersion was obtained using $PdCl_2$ as the palladium source compared to $Pd(NH_3)_2Cl_2$ and $Pd(CH_3COO)_2$ precursors, clearly indicating that differences in dispersion are related to the nature of the Pd precursor. It has been reported that precursors with organic ligands yield lower dispersion than the precursors containing ammonia [13]. The reason is that localized heating due to organic ligand oxidation during calcination may be sufficient to result in sintering of novel metal particles. In addition, metal–support interaction is an important factor that contributes to the overall dispersion on catalysts. For $PdCl_2$ and $Pd(NH_3)_2Cl_2$ it is known that Pd exists as $PdCl_4^{2-}$ and $Pd(NH_3)_4^{2+}$, respectively. Anion exchange reactions between $PdCl_4^{2-}$ and OH^- groups on the support result in strong interaction between Pd species and the support [14,15], which could inhibit metal agglomeration on the surface and result in highly dispersed Pd, as confirmed by particle size data.

H_2-TPR measurements (Fig. 2) clearly demonstrate that the Pd precursor has an important influence on the state of palladium species. In comparison to the TPR profile for the sample prepared using $PdCl_2$, the samples for $Pd(NH_3)_2Cl_2$ and $Pd(CH_3COO)_2$ precursors exhibited a very sharp negative peak at 360 K. This suggests that PdO agglomeration occurred, leading to the formation of large particles that were easily reduced to metallic Pd, for which the characteristic negative TPR peak (360 K) is much larger than that for the sample prepared from $PdCl_2$. In particular, the sample prepared from $Pd(CH_3COO)_2$ exhibited two negative peaks, which may be due to the formation of considerably larger Pd particles. This result is in good agreement with the dispersion and particle size of palladium in Table 2. On the other hand, it is important to note that the Pd precursor has an effect on the state of tungsten, especially polytungstate species, which exhibit a reduction peak at approximately 613 K with intensity decreasing in the order $PdCl_2 > Pd(CH_3COO)_2 > Pd(NH_3)_2Cl_2$.

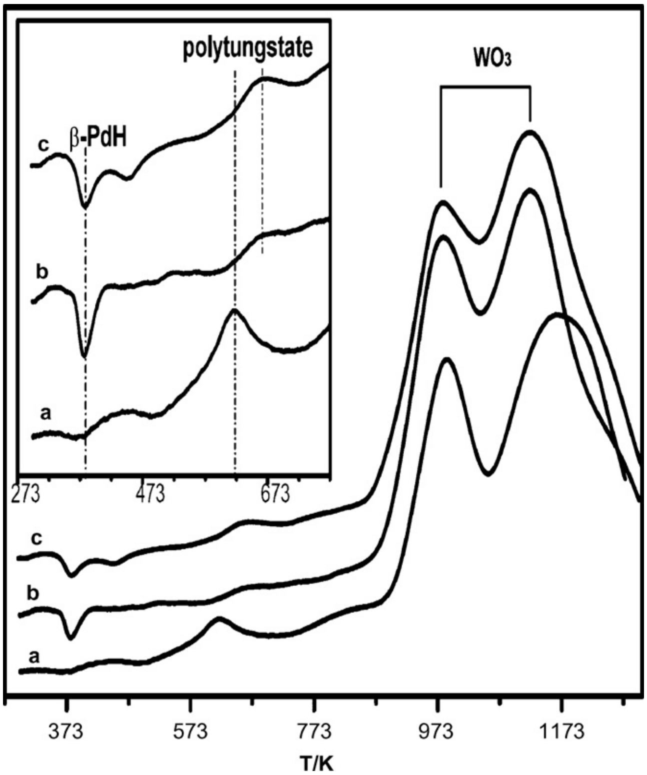

Fig. 2. H_2-TPR spectra of Pd/WO_3–ZrO_2 catalysts prepared with different Pd precursors: (a) $PdCl_2$; (b) $Pd(NH_3)_2Cl_2$; (c) $Pd(CH_3COO)_2$.

Comparison of the catalytic performance of 1.0 wt.% Pd/WO_3–ZrO_2 catalysts for direct oxidation of ethylene reveals a significant difference for different Pd precursors (Table 2). The catalyst prepared from $PdCl_2$ was the most active and selective, with catalytic activity decreasing in the order $PdCl_2 > Pd(CH_3COO)_2 > Pd(NH_3)_2Cl_2$, which is consistent with the order for the reduction peak at 613 K assigned to polytungstate species (Fig. 2). This result further confirms that the catalytic activity of Pd/WO_3–ZrO_2 for selective oxidation of ethylene is strongly dependent on the amount of polytungstate species. In addition, the sample prepared from $PdCl_2$, with the lowest-intensity negative peak at 360 K (Fig. 2) clearly indicating the presence of well-dispersed Pd particles, showed the highest acetic acid

Table 2
Physical properties of 1.0 wt.% Pd/WO_3–ZrO_2 catalysts prepared with different Pd precursors.

Pd precursors	Surface area ($m^2\ g^{-1}$)	Pd dispersion[a] (%)	Pd particle size[a] (nm)	Ethylene conversion (%)	Acetic acid yield ($g\ h^{-1}\ L^{-1}$ cat)	Selectivity (%)		
						Acetic acid	Acetaldehyde	CO_x
$PdCl_2$	39	12.0	9.3	4.2	117	75	11	14
$Pd(NH_3)_2Cl_2$	32	6.4	17.5	1.8	47	65	19	16
$Pd(CH_3COO)_2$	37	0.6	192.5	2.1	59	69	9	22

[a] Calculated from H_2 chemisorption.

selectivity. On the contrary, the catalyst prepared from $Pd(CH_3COO)_2$ precursor showed significantly higher CO_x selectivity, which could be due to the presence of large Pd particles. It is known that, starting from large Pd particles, combustion of ethylene leads to CO_x as the predominant product [16]. The above results suggest that the use of different precursors may result in different Pd species and surface structures that are directly related to the active catalyst sites. Since large Pd particles act as a combustion catalyst, the existence of well-dispersed Pd species appears to be responsible for the higher acetic acid selectivity. Furthermore, the amount of polytungstate species on the ZrO_2 surface, which varied for different Pd precursors, governs the activity of $Pd/WO_3–ZrO_2$ catalysts.

4. Conclusions

In the present study, a series of $Pd/WO_3–ZrO_2$ (W/Zr = 0.2) catalysts with different Pd loadings and precursors prepared by the wet impregnation method was evaluated for selective oxidation of ethylene to acetic acid. The catalytic properties of $Pd/WO_3–ZrO_2$ were strongly influenced by the Pd loading and the type of Pd precursor. For all samples, $Pd/WO_3–ZrO_2$ prepared from a $PdCl_2$ precursor showed the best activity and selectivity. Moreover, the ethylene conversion increased with an increase in Pd loading from 0.5 to 2 wt.%. The results may be due to a higher amount of polytungstate species on the ZrO_2 surface, which was found to play an important role in increasing the catalytic activity of $Pd/WO_3–ZrO_2$ for selective oxidation of ethylene to acetic acid. Furthermore, the catalyst with a larger negative signal in the H_2-TPR profile owing to the presence of larger Pd particles clearly exhibited higher CO_x selectivity, suggesting that well-dispersed Pd species could be responsible for the higher acetic acid selectivity.

Acknowledgements

The authors gratefully acknowledge financial support from the National Science Foundation for Distinguished Young Scholars (Grant No. 20725313) and the Ministry of Science and Technology of China (Grant No. 2005CB221404).

References

[1] S. Takaharu, F. Masayuki, M. Takashige, N. Hiroshi, JP Patent 09-048744 (1997).
[2] S. Takaharu, F. Masayuki, M. Takashige, N. Hiroshi, JP Patent 09-151158 (1997).
[3] C.W. Capp, H.B. Walton, GB Patent 1,142,897 (1969).
[4] K. Sano, H. Uchida, S. Wakabayashi, Catal. Surv. Jpn. 3 (1999) 55.
[5] W.L. Chu, Y. Ooka, Y. Kamiya, T. Okuhara, H. Hattori, Chem. Lett. 34 (2005) 642.
[6] W.L. Chu, Y. Ooka, Y. Kamiya, T. Okuhara, Catal. Lett. 101 (2005) 225.
[7] X.R. Chen, C.L. Chen, N.P. Xu, C.Y. Mou, Catal. Today 93–95 (2004) 129.
[8] H. Lieske, J. Volter, J. Phys. Chem. 89 (1985) 1841.
[9] M. Boudart, H.S. Hwang, J. Catal. 39 (1975) 44.
[10] A. Barrera, J.A. Montoya, M. Viniegra, J. Navarrete, G. Espinosa, A. Vargas, P. del Angel, G. Perez, Appl. Catal. A 290 (2005) 97.
[11] S.R. Vaudagna, S.A. Canavese, R.A. Comelli, N.S. Fígoli, Appl. Catal. A 168 (1998) 93.
[12] D.G. Barton, M. Shtein, R.D. Wilson, S.L. Soled, E. Iglesia, J. Phys. Chem. B 103 (1999) 630.
[13] L.J. Hu, K.A. Boateng, J.M. Hill, J. Mol. Catal. A: Chem. 259 (2006) 51.
[14] R.S. Monteiro, L.C. Dieguez, M. Schmal, Catal. Today 65 (2001) 77.
[15] R. Gopinath, N.S. Babu, J.V. Kumar, N. Lingaiah, P.S.S. Prasad, Catal. Lett. 120 (2008) 312.
[16] W. Unterberger, H. Gabasch, K. Hayek, B. Klotzer, Catal. Lett. 104 (2005) 1.